

A study of V-shaped PTC behaviour of $\text{Sr}_{0.4}\text{Pb}_{0.6}\text{TiO}_3$ ceramics

Zhao Jingchang*, Li Longtu, Gui Zhilun

State Key Laboratory of New Ceramics and Fine Processing, Department of Materials Science and Engineering, Tsinghua University, Beijing, 100084, People's Republic of China

Received 3 April 2001; received in revised form 28 June 2001; accepted 9 July 2001

Abstract

Yttrium-doped $\text{Sr}_{0.4}\text{Pb}_{0.6}\text{TiO}_3$ ceramics were prepared at relatively low sintering temperature using conventional sintering technology. The sintered ceramics exhibit novel NTC–PTC composite effects. The influences of doping PbO and SiO_2 on the properties of $\text{Sr}_{0.4}\text{Pb}_{0.6}\text{TiO}_3$ ceramics were compared. It was found that suitable PbO additives reduce the room-temperature resistivities (ρ_{RT}) of $\text{Sr}_{0.4}\text{Pb}_{0.6}\text{TiO}_3$ ceramics and weaken their NTC effects, but the effect of doping SiO_2 is reverse. The XRD analyses show that SiO_2 additives can cause Pb^{2+} ions segregating out from $\text{Sr}_{0.4}\text{Pb}_{0.6}\text{TiO}_3$ lattices and form PbO· SiO_2 phase. It is estimated that the strong NTC effects of $\text{Sr}_{0.4}\text{Pb}_{0.6}\text{TiO}_3$ ceramics should be closely related to the Pb^{2+} immigration. The domain structure, morphology and compositional distribution of Y-doped $\text{Sr}_{0.4}\text{Pb}_{0.6}\text{TiO}_3$ ceramics were investigated using TEM, SEM and EDAX respectively. The results of EDAX indicate that the Pb/Sr ratio on the grain boundaries is slightly lower than that in the grains. According to the results, the V-shaped PTC behaviors of (Sr,Pb) TiO_3 ceramics are discussed. © 2002 Elsevier Science Ltd. All rights reserved.

Keywords: Electrical conductivity; Electrical properties; NTC; PTC; (Sr,Pb) TiO_3

1. Introduction

Since the V-shaped positive temperature coefficient effect in (Sr,Pb) TiO_3 materials was firstly found in 1988,¹ a lot of research work has been conducted for making known the conduction mechanism of these materials.^{2,3} As a kind of perovskite materials, (Sr,Pb) TiO_3 ceramics exhibit novel NTC–PTC composite effect and sinter at relatively low temperature comparing to the conventional Ba TiO_3 PTCR.^{4,5} Moreover, the Curie temperature of (Sr,Pb) TiO_3 materials can be shifted to higher temperature by increasing Pb^{2+} concentration. Therefore (Sr,Pb) TiO_3 semiconductor ceramics can be used in many apparatus, such as temperature controls, self-regulating heaters and degaussers, especially, as overflow protection devices because (Sr,Pb) TiO_3 V-shaped PTCRs have higher resistivities at room temperature.⁶

At present, (Sr,Pb) TiO_3 V-shaped ceramics are generally prepared using microwave sintering (MS)⁷ and

rapidly thermal sintering (RTS) processing,^{8,9} but these ceramic microstructures are non-equilibrium system, their performances, such as the densification, polarization, dielectric constant and fatigue etc., are deteriorated. Conventional sintering (CS) processing still has advantage of fabricating high performance (Sr,Pb) TiO_3 V-shaped PTCRs, but it is rarely reported.

The Heywang–Jonker model¹⁰ is widely accepted to explain the PTC effect of (Sr,Pb) TiO_3 ceramics above T_c . It is suggested that the abrupt jumps of resistivity above T_c is originated from a barrier on the grain boundary, the height of barrier can be increased rapidly near the Curie temperature because the phase of (Sr,Pb) TiO_3 material changes from tetragonal to cubic structure. As to the NTC effect below T_c , some theories, such as the deep energy level¹¹ and the grain boundary effect,¹² were proposed to interpret the conduction mechanism of (Sr,Pb) TiO_3 materials, but some experimental phenomena still can not be reasonably interpreted. Moreover, D.J. Wang et al.¹³ first prepared the low resistivity (Sr,Pb) TiO_3 -based PTCR with weak NTC effect ($T < T_c$) using chemical synthesis and RTS processing, the results indicated that the intensity of NTC effect can be changed by different ingredients or processing. Therefore, it is significant for practice to

* Corresponding author. Tel.: +86-10-62784579.

E-mail address: zhaojingchang99@mails.tsinghua.edu.cn (J. Zhao).

research and control the NTC effect of (Sr,Pb)TiO₃ ceramics.

In this paper, high-performance Sr_{0.4}Pb_{0.6}TiO₃ V-shaped PTCR were prepared at 1100 °C using conventional sintering processing. The influences of doping PbO and SiO₂ additives on the properties of Sr_{0.4}Pb_{0.6}TiO₃ ceramics were compared. The samples' resistivity-temperature characteristics, Phase structure, microstructure and compositional distribution were investigated respectively to reveal the conduction mechanism of Y-doped Sr_{0.4}Pb_{0.6}TiO₃ thermistors.

2. Experimental

Analytical grade 0.6 mol PbO, 0.6 mol TiO₂, 0.008 mol Y(NO₃)₃ and high purity 0.4 mol SrTiO₃ (decomposed SrTiO(C₂H₄)₂·4H₂O at 1000 °C for 4 h) were mixed and wet-milled in ethanol for 48 h in a plastic jar. After being preheated at 800 °C for 2 h, analytical grade 0.08 mol Si(OC₂H₅)₄ and 0.02 mol PbO were added to the preheated powders respectively and well mixed again, then the mixed powders were pressed into discs with 10mm diameter and about 1mm thickness at pressure of 200 Mpa, then the green pellets were sintered at 1100 °C for 60–90 min in air and cooled at the rate of 4 °C/min.

The surfaces of sintered ceramics were coated with In–Ga alloy and the characteristics of ρ – T were measured from room temperature up to 400 °C with a DC resistance-temperature measuring system. The phase structure of samples was examined using a Regaku D/max IIIB X-ray diffraction meter. The microstructure and compositional distribution were investigated using a Hitachi-800 transmission electron microscope (TEM) and a JSM-6301F scanning microscope (SEM) with energy dispersive analysis of X-ray (EDAX) respectively.

3. Results and discussion

The resistivity-temperature curves of Sr_{0.4}Pb_{0.6}TiO₃ + 0.8 mol% Y³⁺ ceramics sintered at 1100 °C for different times are shown in Fig. 1. The samples exhibit low room temperature resistivities (ρ_{RT}) and NTC–PTC composite characteristics. With elevating measuring temperature, the samples' resistivities decrease more than one order of magnitude in the NTC effect region ($T < T_c$) and jump about five orders of magnitude in the PTC effect region ($T > T_c$). At the same time, the samples' ρ_{RT} increase and their NTC effects ($T < T_c$) become stronger with increasing the soaking time.

In general, Sr_xPb_{1-x}TiO₃ ceramics with NTC–PTC composite effects were fabricated by glass/ceramic composing.⁹ The strong NTC–PTC composite effects were

demonstrated to originate from the electrical behavior of grain boundary according to the complex impedance analysis.^{3,13} In this article, 2 mol% PbO and 8 mol% Si(OC₂H₅)₄ were doped into preheated Y-doped Sr_{0.4}Pb_{0.6}TiO₃ powders respectively and the influences of PbO and SiO₂ additives on the properties of (Sr,Pb)TiO₃ thermistors were investigated. Fig. 2 gives the resistivity-temperature curves of samples sintered at 1100 °C for 1 h. All samples in Fig. 2 exhibit strong

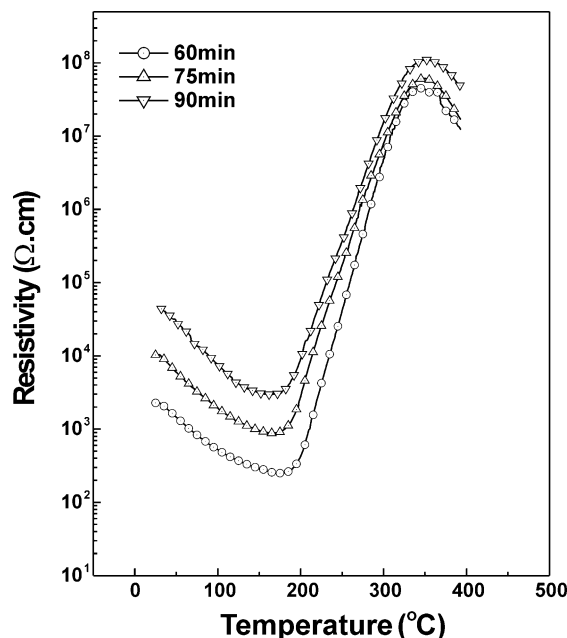


Fig. 1. Resistivity-temperature curves of Sr_{0.4}Pb_{0.6}TiO₃ ceramics sintered at 1100 °C for 60, 75 and 90 min.

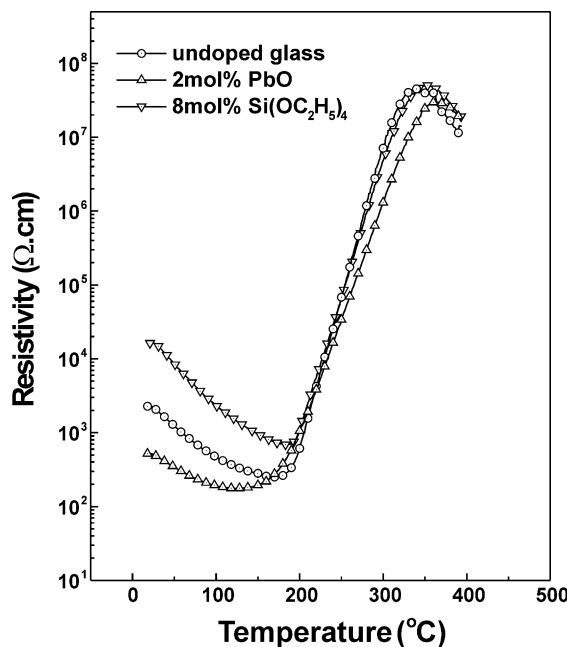


Fig. 2. Resistivity-temperature curves of Sr_{0.4}Pb_{0.6}TiO₃ ceramics sintered at 1100 °C for 1 h.

PTC behaviors ($T > T_c$), their resistivities jump more than 4.5 orders of magnitude in the PTC effect regions. The sample's ρ_{RT} (undoped glass) is $2.2 \times 10^3 \Omega\text{-cm}$ and its resistivity variability $\log(\rho_{RT}/\rho_{min})$ in the NTC effect region is near 1.0 order of magnitude. Furthermore, the ρ_{RT} and NTC effects ($T < T_c$) are changed with doping different impurities. The sample's ρ_{RT} and $\log(\rho_{RT}/\rho_{min})$ at doping 2 mol% PbO reduce to $4.78 \times 10^2 \Omega\text{-cm}$ and 0.45 order of magnitude respectively. On the contrary, the sample's ρ_{RT} and $\log(\rho_{RT}/\rho_{min})$ at doping 8 mol% $\text{Si}(\text{OC}_2\text{H}_5)_4$ increase to $1.57 \times 10^4 \Omega\text{-cm}$ and 1.38 order of magnitude respectively.

The XRD patterns of sintered samples corresponding to those in Fig. 2 are shown in Fig. 3. It can be seen that the samples have typical tetragonal crystal structure, and the ratio c/a can be calculated by (002) and (200) diffraction peaks, its value is about 1.015. The obvious diffraction peaks corresponding to $\text{PbO}\cdot\text{SiO}_2$ phase (marked *) only appeared in the sample with doping 8

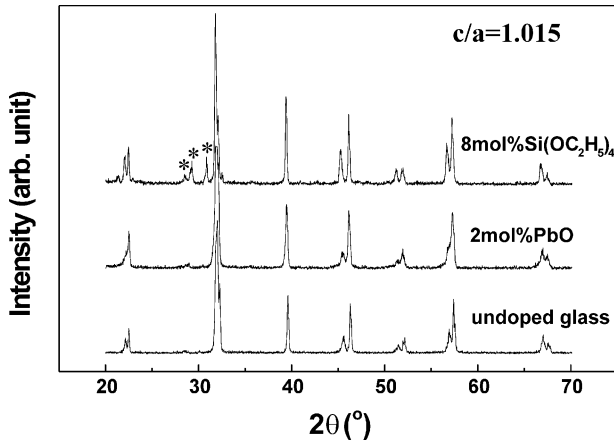


Fig. 3. XRD patterns of $\text{Sr}_{0.4}\text{Pb}_{0.6}\text{TiO}_3$ ceramics sintered at 1100°C for 1 h.

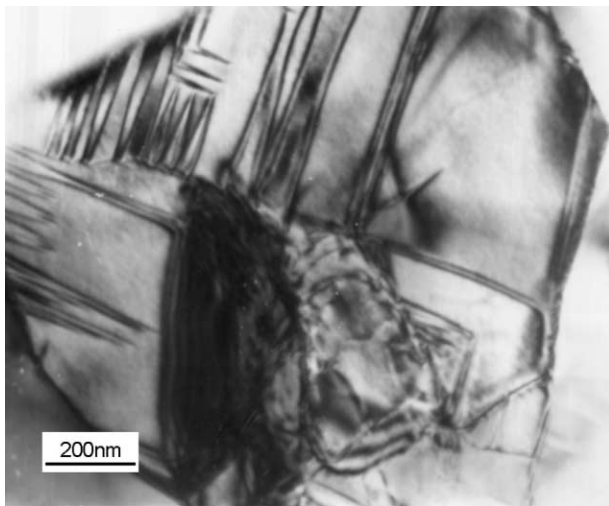


Fig. 4. TEM micrograph of $\text{Sr}_{0.4}\text{Pb}_{0.6}\text{TiO}_3 + 0.8 \text{ mol\% } \text{Y}^{3+}$ ceramic sintered at 1100°C for 1 h.

mol% $\text{Si}(\text{OC}_2\text{H}_5)_4$. The results indicate that a small amount of Pb^{2+} ions separated out from $\text{Sr}_{0.4}\text{Pb}_{0.6}\text{TiO}_3$ lattices and dissolved into the glass phase during sintering.

A “core-shell” microstructure model in SiO_2 -doped $(\text{Sr,Pb})\text{TiO}_3$ ceramics has been reported using microwave sintering (MS) or rapid thermal sintering (RTS) processing.^{7,8} According to the results of EDAX, it was suggested that $(\text{Sr,Pb})\text{TiO}_3$ ceramics contains grains of “core-shell” microstructure, the Pb-deficient core is packed by the Pb-enriched perovskite $(\text{Sr,Pb})\text{TiO}_3$ and the electrical behavior of the core is completely shielded. The thickness of the shell varies with the temperature below the Curie temperature, which results in a strong NTC effect. In our experiments, Figs. 1 and 2 show that Y-doped $\text{Sr}_{0.4}\text{Pb}_{0.6}\text{TiO}_3$ ceramics without SiO_2 additives also exhibit strong V-shaped PTC behaviors. 2 mol% PbO additives decrease the ceramic ρ_{RT} and $\log(\rho_{RT}/\rho_{min})$ and 8 mol% $\text{Si}(\text{OC}_2\text{H}_5)_4$ additives increase the ceramic ρ_{RT} and $\log(\rho_{RT}/\rho_{min})$. Furthermore, the XRD analyses in Fig. 3 show that SiO_2 additives result in the Pb^{2+} immigration. Therefore, it is assumed that the variation of Pb^{2+} concentration in $\text{Sr}_{0.4}\text{Pb}_{0.6}\text{TiO}_3$ ceramics forms some acceptor defects on the grain boundary, which is primary factor to cause the NTC behaviors below T_c .

Fig. 4 gives the TEM micrograph of $\text{Sr}_{0.4}\text{Pb}_{0.6}\text{TiO}_3 + 0.8 \text{ mol\% } \text{Y}$ ceramic sintered at 1100°C for 1 h. It shows, from Fig. 4, that the grains have obvious electrical domains and that most domains have a parallel or vertical distribution with each other. This domain distribution is beneficial to releasing thermal stress during phase transformation. At the same time, this domain structure indicates the grains are composed of ferroelectric phase.

SEM and EDAX were also employed to investigate the microstructure and compositional distributions of samples. The morphology of sintered surface and fracture are shown in Fig. 5(a) and (b) respectively. It can be seen from Fig. 5(a) that the sizes of most grains on the ceramic surface are in the range of 2–5 μm . Fig. 5(b) shows that the ceramic ruptures partly through the grains, others rupture along the grain boundaries. The samples' compositional distributions in the grains and grain boundaries were respectively measured using EDAX and the results are shown in Fig. 5(c) and (d). By comparison, it can be seen that the intensive ratio of $\text{Sr}_{L\alpha}/\text{Pb}_{L\alpha}$ in Fig. 5(d) is slightly larger than that in Fig. 5(c). After simulate calculation, the content ratio of Sr/Pb in the grains is 1.20:1.00 and that at the grain boundaries is 1.34:1.00. It confirms that the Pb concentration at the grain boundaries is slightly lower than that in the grains. The grain boundaries of samples are composed of Pb-deficient perovskite. This microstructure accords with the proposed model in literature.¹⁴

As a donor, trivalent Y^{3+} ions ($r_{\text{Sr}^{2+}} = 0.89 \text{ \AA}$) preferentially substitute Sr^{2+} ($r_{\text{Sr}^{2+}} = 1.16 \text{ \AA}$) or Pb^{2+}

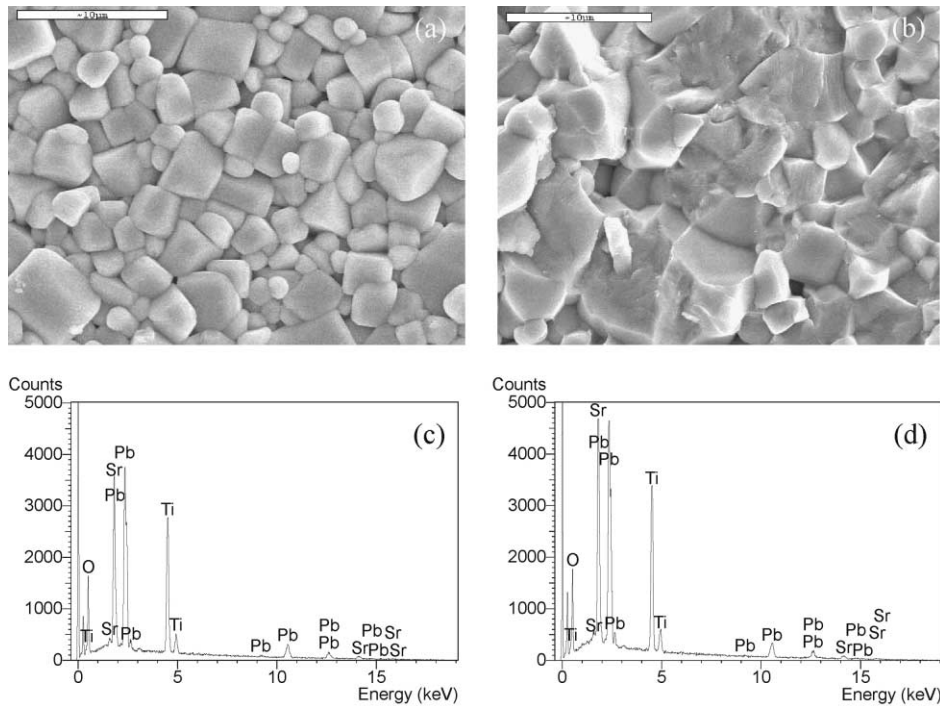
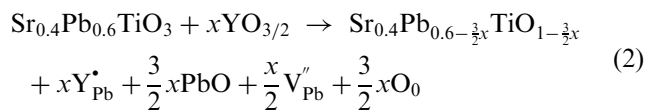
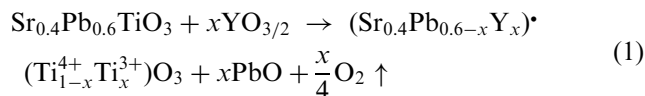


Fig. 5. SEM micrographs of $\text{Sr}_{0.4}\text{Pb}_{0.6}\text{TiO}_3 + 0.8 \text{ mol}\% \text{ Y}^{3+}$ ceramic sintered at 1100°C for 1 h: (a) surface, (b) fracture and the EDS spectra: (c) grains, (d) grain boundaries.

($r_{\text{Pb}^{2+}} = 1.18 \text{ \AA}$) in $\text{Sr}_{0.4}\text{Pb}_{0.6}\text{TiO}_3$ lattices to form defects Y_{Sr}^{\bullet} or Y_{Pb}^{\bullet} .⁶ However the phase diagrams show that the melting temperature of PbTiO_3 ($\text{mp} \approx 1285^\circ\text{C}$) is much lower than that of SrTiO_3 ($\text{mp} \approx 2040^\circ\text{C}$) and PbO loss by volatilization is difficult to be avoided during calcination.³ Therefore, it is assumed that Pb^{2+} ions in $\text{Sr}_{0.4}\text{Pb}_{0.6}\text{TiO}_3$ lattices should mainly be substituted by Y^{3+} ions. The redundant charges can be compensated for by two ways: (i) Ti^{4+} ions are reduced as Ti^{3+} ions. (ii) form cationic vacancies, e.g. $V_{\text{Pb}}^{\prime\prime}$. Both defect reactions can be described as follow:



According to above formulae, PbO loss will cause (i) a move to the right, which is beneficial to improving the semiconduction of $\text{Sr}_{0.4}\text{Pb}_{0.6}\text{TiO}_3$ materials by producing more Ti^{3+} ions. However, overmuch PbO loss also causes (ii) a move to the right and formation of large Pb vacancies to compensate the defects Y_{Pb}^{\bullet} . The defect complex $(V_{\text{Pb}}^{\prime\prime} \cdot 2Y_{\text{Pb}}^{\bullet})^x$ declines the effect of donor Y^{3+} ions. Therefore, a suitable amount of PbO additives will compensate the PbO loss in $\text{Sr}_{0.4}\text{Pb}_{0.6}\text{TiO}_3$ lattices during calcination and benefit to decrease the resistivity of

$(\text{Sr,Pb})\text{TiO}_3$ materials at room temperature. It well explains the samples' resistivity-temperature behaviors in Figs. 1 and 2.

Y -doped $\text{Sr}_{0.4}\text{Pb}_{0.6}\text{TiO}_3$ V-shaped PTCR is a kind of n -type perovskite ceramics, whose electrical conduction significantly depends on the leap of electrons among the Ti^{4+} ions under an electric field. The conduction of $\text{Sr}_{0.4}\text{Pb}_{0.6}\text{TiO}_3$ ceramics in the NTC effect region should be controlled by the charge carriers of perovskite $(\text{Sr,Pb})\text{TiO}_3$ structure similar to that in the PTC region. However cationic vacancies, especially Pb^{2+} vacancies $V_{\text{Pb}}^{\prime\prime}$ will be disadvantageous to forming Ti^{3+} ions in $(\text{Sr,Pb})\text{TiO}_3$ polycrystalline because the donor defects Y_{Pb}^{\bullet} have been compensated.⁶ With $V_{\text{Pb}}^{\prime\prime}$ concentration increasing, the defect complexes $(V_{\text{Pb}}^{\prime\prime} \cdot Y_{\text{Pb}}^{\bullet})$ in $(\text{Sr,Pb})\text{TiO}_3$ ceramics increase and result in high ρ_{RT} . Of course, the constraint to forbid partial Ti^{4+} ions participating in electrical conduction will be impaired with the elevating temperature. So the samples' resistivities decrease sharply below T_c (NTC effects).

4. Conclusions

A kind of V-shaped PTCR based on $\text{Sr}_{0.4}\text{Pb}_{0.6}\text{TiO}_3$ materials was fabricated by conventional sintering methods. The influence of some glass on the properties of $\text{Sr}_{0.4}\text{Pb}_{0.6}\text{TiO}_3$ materials was investigated, SiO_2 additives cause Pb^{2+} segregation and form a $\text{PbO} \cdot \text{SiO}_2$ phase, which is beneficial to increasing room-temperature

resistivities of $\text{Sr}_{0.4}\text{Pb}_{0.6}\text{TiO}_3$ ceramics and enhancing their NTC effects below T_c . On the contrary, doping a small amount of PbO decreases the sample's ρ_{RT} and NTC effects. The compositional distributions of samples without doping glass were measured using EDAX, the results confirm that Pb/Sr ratio on the grain boundaries is slightly smaller than that in the grains. Therefore it is assumed that the electrical properties of $\text{Sr}_{0.4}\text{Pb}_{0.6}\text{TiO}_3$ ceramics should be significantly affected by Pb^{2+} immigration and the strong NTC effect of (Sr,Pb)TiO₃ ceramics below T_c might be closely related to the Pb^{2+} vacancies at the grain boundaries.

Acknowledgements

Authors are grateful to Qi Jianquan and Zhang Ningxin for their help and valuable discussion.

References

1. Hamata, Y., Takuchi, H. and Zomura, K. Jpn. Patent No. 63-280401, 1988.
2. Lee, C., Lin, I.-N. and Hu, C.-T., Evolution of microstructure and V-shaped positive temperature coefficient of resistivity of $(\text{Pb}_{0.6}\text{Sr}_{0.4})\text{TiO}_3$ materials. *J. Am. Ceram. Soc.*, 1994, **77**(5), 1340–1344.
3. Lu, Y.-Y. and Tseng, T.-Y., Electrical characteristics of $(\text{Pb,Sr})\text{TiO}_3$ positive temperature coefficient ceramics. *Materials Chemistry and Physics*, 1998, **53**, 132–137.
4. Er, G., Ishida, S. and Takeuchi, N., Investigations of the electrical property, diffuse reflectance and ESR spectra of the La-(Fe,Mn)-codoped PTCR BaTiO_3 annealed in reducing atmosphere. *J. Mater. Sci.*, 1999, **34**, 4265–4270.
5. Kutty, T. R. N. et al., Effect of charge redistribution through secondary phase formation on PTCR characteristics of $n\text{-BaTiO}_3$ ceramics. *Materials Letters*, 1998, **34**, 43–49.
6. Lee, C., Lin, I.-N. and Hu, C.-T., Evolution of microstructure and V-shaped positive temperature coefficient of resistivity of $(\text{Pb}_{0.6}\text{Sr}_{0.4})\text{TiO}_3$ materials. *J. Am. Soc.*, 1994, **77**(5), 1340–1344.
7. Chou, C.-C., Chang, H.-Y. and Lin, I.-N. et al., Microscopic examination of the microwave sintered $(\text{Pb}_{0.6}\text{Sr}_{0.4})\text{TiO}_3$ positive-temperature-coefficient resistor materials. *Jpn. J. Appl. Phys.*, 1998, **37**, 5269–5272.
8. Cheng, H.-F., Hu, C.-T. and Lin, Y.-Y. et al., Modeling on the resistivity-temperature properties of $(\text{Pb}_{0.6}\text{Sr}_{0.4})\text{TiO}_3$ materials prepared by the rapid thermal sintering process. *Jpn. J. Appl. Phys.*, 1998, **37**, 1932–1938.
9. Wang, D. J., Qiu, J. and Gui, Z. L. et al., Design for high-performance functional composite thermistor materials by glass/ceramic compositing. *J. Mater. Res.*, 1999, **14**(7), 2993–2996.
10. Heywang, W., Barium titanate als sperrschichtbleiter. *Solid State Electronics*, 1961, **44**(3), 51–58.
11. Iwaya, S., Masumura, H., Taguchi, H. and Hamada, M., *J. Electron. Ceram. Jpn.*, 1988, **19**, 33.
12. Wang, D. J., Gui, Z. L. and Li, L. T., Preparation and electrical properties of semiconducting strontium lead titanate PTCR ceramics. *J. Mater. Sci.: Materials in Electronics*, 1997, **8**, 271–276.
13. Wang, D. J., Qiu, J., Guo, Y. C., Gui, Z. L. and Li, T. L., Grain boundary effects in NTC–PTC composite thermistor materials. *J. Mater. Res.*, 1999, **14**(1), 120–123.
14. Chang, H. Y., Liu, K. S. and Chen, H. W. et al., V-shaped positive temperature coefficient of resistivity (PTCR) characteristics of microwave-sintered $(\text{Sr}_{0.4}\text{Pb}_{0.6})\text{TiO}_3$. *Mater. Chem. Phys.*, 1995, **42**, 258–263.